NATIONAL ADVISORY COMMITTEE FOR AERONAUTICS

WARTIME REPORT

ORIGINALLY ISSUED

May 1945 as
Advance Confidential Report 5D04

FLIGHT INVESTIGATION OF THE VARIATION OF DRAG COEFFICIENT

WITH MACH NUMBER FOR THE BELL P-39N-1 AIRPLANE

By Welko E. Gasich and Lawrence A. Clousing

Ames Aeronautical Laboratory
Moffett Field, California

NACA

WASHINGTON

NATIONAL ADVISORY COMMITTEE FOR AERONAUTICS

ADVANCE CONFIDENTIAL REPORT

FLIGHT INVESTIGATION OF THE VARIATION OF DRAG COEFFICIENT

WITH MACH NUMBER FOR THE BELL P-39N-1 AIRPLANE

By Welko E. Gasich and Lawrence A. Clousing

SUMMARY

An investigation of the effect of compressibility on the drag of a Bell P-39N-1 airplane has been made in flight as part of a drag study on several high-speed airplanes currently in production. The Mach number range covered in these tests was from 0.2 to about 0.8.

The minimum drag coefficient at low Mach number was found to be 0.022. The drag coefficient started to increase at a Mach number of 0.62, reaching a value almost three times as great at a Mach number of 0.80. From the results of the tests it appears that the terminal Mach number for the airplane during a dive from service ceiling is about 0.80.

INTRODUCTION

One of the compressibility effects which occurs on airplanes in flight at speeds approaching those of the speed of sound is that of a large increase in the airplane drag coefficient. The Mach number at which this drag increase occurs, and the ability to predict its magnitude, is a subject of intense research at present, because the high-speed performance of modern airplanes is affected by the nature of the drag increase. Also, the terminal dive speed of airplanes is determined to a large extent by the nature of the increase of drag at high Mach numbers. At present, reliable full-scale data on the drag characteristics of airplanes at high Mach numbers are quite limited.

As a result, the Ames Aeronautical Laboratory has undertaken drag investigations in flight of several high-speed airplanes currently in production. The present investigation was conducted to determine the manner in which the drag coefficient of a Bell P-39N-1 airplane varied with Mach number. Measurements were taken up to the highest value of Mach number attainable.

In conducting the investigation, it was found necessary to devote special study to the technique for the determination of drag characteristics of airplanes in flight. A description is presented herein of the methods used, and the results obtained through the use of different methods of computing the drag are compared.

SYMBOLS

In the derivation of the formulas by which the drag coefficient is obtained, the following symbols are used:

F total force parallel to flight path acting to accelerate the airplane, pounds

s distance through which force acts, feet

m mass of airplane, W/g, pound-seconds squared per foot

W weight of airplane, pounds

a acceleration of airplane along flight path (in direction of F), feet per second squared

g acceleration due to gravity, feet per second squared

h true altitude, feet

V true airspeed, miles per hour

D total drag of airplane, pounds

q dynamic pressure, pounds per square foot

S wing area, square feet

T   total thrust, pounds

A_X the algebraic sum of the components along the airplane
        X-axis of the airplane acceleration and the accelera-
        tion due to gravity in terms of the standard gravi-
        tational unit (32.2 ft/sec²), positive when directed
        forward

A_{X_1} longitudinal acceleration factor due to attitude of air-
        plane in terrestrial gravitational field

A_{X_2} longitudinal acceleration factor due to acceleration of
        airplane through space

A_Z the algebraic sum of the components, along the airplane
        Z-axis, of the airplane acceleration and the accel-
        eration due to gravity, in terms of the standard
        gravitational unit (32.2 ft/sec²), positive when di-
        rected upward

A_{Z_1} normal acceleration factor due to attitude of airplane
        in terrestrial gravitational field

A_{Z_2} normal acceleration factor due to acceleration of air-
        plane through space

θ angle of flight path as measured from horizontal, degrees

α angle of attack of thrust line, degrees

M   Mach angle

DESCRIPTION OF THE AIRPLANE

The Bell P-39N-1 airplane is a single-place, low-wing,
cantilever monoplane powered by a 1200 brake horsepower (take-
off rating) Allison V-1710-85 liquid-cooled engine driving a
three-blade Aeroproducts propeller. Figure 1 is a general-
arrangement drawing of the airplane. Figure 2 is a photograph
of the airplane as instrumented for the flight tests. The
following specifications of the airplane were taken almost en-
tirely from references 1 and 2:

Airplane, general

    Span . . . . 34.0 ft

    Length . . . . 30.167 ft

    Weight (normal and approx. as flown) . 7629 lb

    Center of gravity (for normal gross
       weight and approx. as flown). . . . 0.285 M.A.C.

Wing

    Airfoil section, root . . . . NACA 0015

    Airfoil section, tip . . . . NACA 23009

    Area . . . . 213.2 sq ft

Engine

    Type . . . . Allison V-1710-85

    Ratings   (bhp/rpm/altitude)

        Take-off . . . . 1200/3000/sea level
        Military 1125/3000/15,500
        Normal 1000/2600/14,000

    Gear ratio 2.23:1

Propeller

    Type . . . . Aeroproducts,
                                   constant-speed,
                                   hollow-shaft

    Blade design A-20-156-17

    Number of blades 3

    Activity factor/blade 98.5

    Thickness ratio, 75-percent radius . . 0.08

    Diameter . . . . 11 ft, 7 in.

INSTRUMENTATION

Standard NACA instruments were used to record photographically, as a function of time, quantities from which the following variables could be obtained: indicated airspeed, pressure altitude, normal acceleration, longitudinal acceleration, engine manifold pressure, engine speed, and approximate angle of attack of the thrust line. The instrument for measuring longitudinal acceleration was made especially sensitive for the purpose of the tests.

The recording instruments, as installed in the airplane, could be read to ±2 miles per hour for the indicated airspeed, ±200 feet for the altitude, ±0.1g for the normal acceleration, ±0.01g for the longitudinal acceleration, ±0.2 inch of mercury for the manifold pressure, ±20 rpm for the engine speed, and ±0.2° for the angle of attack.

The temperature was measured by the pilot's service thermometer. Temperature surveys were made in ascending and descending flight in an effort to eliminate errors in temperature reading caused by the lag effect in the system. The average temperature read was corrected for the temperature rise caused by the compression of the air due to the speed of the airplane.

The head used for the airspeed and altitude measurements was freely swiveling and was mounted on the end of a boom extending about 4 feet ahead of the leading edge of the right wing at a spanwise location about 7 feet inboard of the right wing tip. The airspeed head consisted of two separate static-pressure tubes (one of which was connected to the airspeed recorder and the other to the altitude recorder) with a single total-pressure tube located between them. The airspeed and altitude recorders were mounted in the right wing at the base of the boom. The total- and static-pressure lines to the airspeed recorder were balanced so that a sudden pressure change equally applied to both total- and static-pressure lines at the airspeed head caused no reading of the airspeed recorder. The lines to the airspeed recorder and altitude recorder were of about the same length and size, being about 5 feet long and of 0.12 inch inside diameter. The magnitude of the lag effects in the altitude and airspeed recording systems was measured by a specially built ground setup, and was found in both systems to be smaller than an error in pressure equivalent to 5 feet of altitude with the airplane in a dive at

terminal Mach number. The recording and service static heads
were calibrated for position error by comparing the readings
of the recording and service altimeters with the known pres-
sure altitude as the airplane was flown at several speeds past
a reference height. It was assumed that the correct total
pressure was obtained. Calibration of the recording head in
the Ames 16-foot wind tunnel showed that the error in recorded
airspeed, due to the difference in Mach number between the
highest value obtained in the flight calibration (0.50) and
the highest value obtained in the flight tests (0.80), was less
than 1 percent. Indicated airspeed, as used in this report,
was computed according to the formula by which standard air-
speed meters are graduated (gives true airspeed at standard
sea-level conditions). The formula may be written as follows:

$$V_i = 1703 \left[\left(\frac{H-p}{p_0} + 1 \right)^{0.286} -1 \right]^{1/2}$$

where

V   correct indicated airspeed, miles per hour

H   free-stream total pressure

p   free-stream static pressure

p_0 standard atmospheric pressure at sea level

The angle of attack of the thrust line was indicated by
a vane mounted on the forward end of a boom located at a span-
wise station 6.7 feet inboard from the left wing tip and ex-
tending 3.3 feet ahead of the wing leading edge similar to the
airspeed-head installation. The angle of attack as measured
by this vane was used in this analysis without any corrections
being applied for position error.

METHODS OF ANALYSIS

It was found necessary in the course of these analyses,
as will be explained later, to calculate drag coefficient from
high-speed-dive data for Mach numbers above 0.5 and from speed-
power data for Mach numbers below this figure. Three differ-
ent methods were applied to the dive data, while a single meth-
od was applied to the speed-power data.

The methods which were applied to the dive data will be referred to in this report as (1) force method, (2) energy method, and (3) acceleration method. The equations derived in appendix A are as follows:

(1) Force method

$$C_D = \frac{T \cos \alpha - W \left[\dfrac{dh/dt}{V} + \dfrac{dV/dt}{g} \right]}{qS}$$

(2) Energy method

$$C_D = \frac{T \cos \alpha - \dfrac{W}{V} \dfrac{d}{dt} \left[h + \dfrac{V^2}{2g} \right]}{qS}$$

(3) Acceleration method

$$C_D = \frac{T \cos \alpha + W(A_Z \sin \alpha - A_X \cos \alpha)}{qS}$$

The equations shown in the foregoing for the force and energy methods are identical except for form. It was felt that a distinction should be made, however, in order to emphasize the significance of the terms within the brackets. Also, the implied differentiations were advered to in applying the equations.

The foregoing methods yielded poor results when applied to test data where the Mach number was below 0.5; therefore, another method was developed which was applicable to data obtained during speed-power runs in level flight. This method is discussed in appendix B, but is not completely derived because of the rather lengthy series of computations involved.

In evaluating the total thrust developed by the engine-propeller combination, it was necessary to include both the exhaust thrust and propeller thrust. The exhaust thrust was estimated by the method used in reference 3 and the propeller

thrust was determined from estimations of propeller efficiency
and engine power. Propeller efficiency was estimated by the
method described in appendix C using charts and data presented
in references 4, 5, and 6.

The engine brake horsepower was determined from the manu-
facturer's engine-power charts by entering readings of the re-
cording altimeter, rpm recorder, and manifold pressure recorder.
In many instances, the manifold pressure at given altitude and
engine-speed conditions exceeded that shown by the engine-power
charts. In such cases it was assumed that a line of constant
rpm and manifold pressure could be extrapolated linearly to the
higher altitude to determine engine power. It might be pointed
out that this assumption is not exactly true, because the ad-
ditional manifold pressure is not supplied by the gear-driven
supercharger within the engine but by the ram effect in the fuel-
induction system; hence, the manifold pressure is not obtained
entirely by the expenditure of power in the supercharger. The
amount of ram pressure is, however, such a small percentage of
the total manifold pressure that it was believed that no seri-
ous errors resulted from this assumption.

                    TESTS, RESULTS, AND DISCUSSION

The data were obtained in high-speed dives and in speed-
power runs with the airplane in the clean condition with oil
and coolant shutters one-half open (flush with the external
lines of fuselage). Pressure orifices were present in the
empennage and right wing, having been placed there for other
test purposes, and an extra aerial mast was mounted ahead of
the cockpit canopy. A research angle-of-attack head and boom
was mounted on the left wing and a research airspeed head and
boom was mounted on the right wing. A bomb rack and sway
braces were mounted under the center of the fuselage. In or-
der to insure that the landing-wheel doors did not open at
high speeds and pull-outs, special latches were installed so
that the doors were positively locked during flight. A list
of the dives involved in these tests and the approximate
flight conditions during the dives are presented in table I.

In order that the force, energy, and acceleration methods
of determining the drag coefficient could be compared in re-
gard to accuracy and consistency, two dives, the time his-
tories of which are shown in figures 3(a) and 3(b), were ana-
lyzed by each of the methods.

Figure 3(a) shows a time history of a power-on dive (dive
No. 1 of table I) from 30,000 feet at full throttle and 3050
rpm. The maximum indicated airspeed reached was 464 miles per
hour at 12,500 feet. The maximum Mach number reached in the
dive was 0.765. The airplane was pulled out at 11,500 feet
at a normal acceleration of 6.0g. It should be noticed that
the manifold pressure kept rising constantly until a value of
50 inches of mercury was reached, at which point there was a
sharp break and the pressure became constant. This break was
due to the pilot's throttling back in order to keep the mani-
fold pressure below the maximum permissible value of 51 inches
of mercury.

Figure 3(b) shows time history of a power-on dive (dive
No. 2 of table I) from 28,000 feet at part throttle and 2800
rpm. The maximum indicated airspeed reached in this dive was
471 miles per hour at 10,300 feet. The maximum Mach number
reached was 0.777. The reason for the sudden decrease in manifold
pressure at the beginning of the dive is due to loss of power
caused by malfunctioning of the fuel-induction system of the
engine when negative accelerations are incurred.

The airplane drag coefficient calculated from the data
obtained in the dive shown in figure 3(a), as determined by
the three methods of evaluation, is shown in figure 4(a) with
airplane drag coefficient C_D plotted as a function of Mach
number M. The results are presented only for Mach numbers
above 0.6. The variation of C_D with M as determined by
the acceleration method appears to be the most reasonable
variation of those shown. The energy and force methods are
consistent within themselves to a small degree, but are in no
way consistent with the acceleration method. The drag-coef-
ficient curves determined by the force and energy methods,
in fact, show an illogical variation with Mach number.

An attempt was made to investigate the reason for this
variation by assuming that the curve of C_D plotted as a
function of Mach number as determined by the acceleration
method was correct. From this curve the data were worked
backward until a time history of the true airspeed was deter-
mined. A comparison of the actual variation of airspeed with
time that was obtained from the data showed that in no case
was there a difference of more than 5 miles per hour true
airspeed. This error in measurement of true airspeed is en-
tirely possible, especially when it is realized that in deal-
ing with true airspeed an accurate temperature measurement is
necessary to obtain true airspeed from indicated airspeed.

Hence, it would appear that inherently the energy and force
methods are too sensitive to minor errors in the measurement
of airspeed to make the methods usable in flight work.   The
inconsistency between force and energy methods may be due to
the fact that for the force method two graphical differenti-
ations are necessary, one to determine the dive angle and the
other to determine the longitudinal acceleration, while only
one differentiation is necessary for the energy method.

        The drag results of the dive of figure 3(b) are shown
on figure 4(b).   In this case the results of the energy and
force methods do not agree with each other as well as in the
previous example, although in this case the energy and force
methods give lower drag coefficients at Mach numbers less
than 0.71 as compared to values presented in figure 4(a).

        Because of the apparent inconsistency of results obtained
by the energy and force methods, all the dive data were finally
derived by the acceleration method.   These data are shown in
figure 5.   The results are consistent and the test points de-
termine a well-defined curve of drag coefficient as a function
of Mach number for a lift-coefficient range of 0.03 to 0.09.
The greatest inaccuracy in computed drag coefficient at the
high Mach numbers should not exceed 2 percent, because the en-
gine thrust (propeller and exhaust) does not exceed 7 percent
of the total drag at these Mach numbers.   The possible error
rises, however, at low Mach numbers, due to the value of the
thrust more closely approaching that of the drag.   At a Mach
number of 0.5, the thrust is equal to the drag.

        The drag coefficients at Mach numbers below 0.5 have been
calculated by the method outlined in appendix B and are shown
in figure 5.   To obtain data for this method, the airplane was
flown in straight level flight at various power conditions at
an altitude of 15,000 feet, thus obtaining a speed-power curve
for the airplane.   The results of the data after they were re-
duced and plotted as figure 6 indicate an airplane drag co-
efficient of 0.022 at a lift coefficient of zero, which seems
to be a reasonable figure, since the particular airplane tested
was aerodynamically rather unclean.

        It is of interest to note in figure 5 that one of the
points plotted was obtained from dive data during a time in
the dive recovery in which the Mach number was decreasing after
having reached a high value.   The position of this point above

the general curve may possibly be attributed to a hysteresis effect caused by the continuance of compressibility stall on some portion of the airplane following flight at high Mach number. It may also have been caused by increased bulging or distortion of the surface of the airplane as it dived into the lower atmosphere where a larger value of dynamic pressure occurs at a given Mach number than is the case at high altitude.

Data are presented in figure 5 on the section critical Mach numbers (the flight Mach number at which the local air-speed over the surface reaches sonic velocity) for various spanwise stations on the wing of the airplane. The various spanwise stations at which the section critical Mach number of the wing was determined are shown in figure 7. The variation of wing thickness with span is also shown in this figure. The values of critical Mach number of each of the spanwise stations shown in figure 7 were determined as described in appendix D and are shown in figure 8. The pressure-distribution measurements used in determining the critical Mach number of each spanwise station were obtained during the flight tests reported in reference 7, and are on file at Ames laboratory. The critical Mach number for the four approximately symmetrical inboard sections (0015 to 0012) is about 0.68. The critical Mach number for the tip section (23010) is much lower than that for the symmetrical sections, because the tip section is operating at a lift coefficient less than the optimum lift coefficient for maximum critical Mach number. The values of wing critical Mach number are spotted on figure 5 to show their relation to the airplane Mach number of drag divergence. (Drag divergence is defined as the point at which the drag coefficient begins to increase over its low speed value.)

It is seen that the drag coefficient starts increasing at a Mach number of 0.62, about 0.03 higher than the tip-section critical Mach number. The critical Mach number on the rest of the wing is not reached, however, until approximately 0.06 Mach number after the airplane Mach number of drag divergence is reached. It is probable that shock waves developing on parts of the airplane (e.g., canopy, duct entrances, etc.), other than the wing tip, contribute to the early drag increase.

It is interesting to notice that the value of dC_D/dM keeps gradually increasing up to a Mach number of 0.75. The value of dC_D/dM between Mach numbers of 0.75 and 0.80 is approximately 0.5.

The highest Mach number reached in any dive was about 0.8 which appears to be the terminal Mach number for the Bell P-39N-1 airplane when dived power on from its service ceiling. No difference in the maximum Mach number attainable was discerned between dives where the entry was made by rolling over into the dive and those in which entry was made by pushing down into the dive. Calculations of the terminal Mach number which could be reached in a vertical dive from 34,000 feet to sea level were made by a step-by-step process using the drag curve of figure 5 with a slight extrapolation. Since at high Mach numbers the propeller thrust in power-on flight is a very small proportion of the total thrust component, the effect of the propeller thrust was neglected in these computations. The results indicated that the highest Mach number would be obtained at an altitude of about 19,000 feet and that this Mach number would be 0.802, which is but slightly higher than the maximum Mach number obtained in the drag tests. The computations indicated a decrease in Mach number as the airplane continued the dive below 19,000 feet.

The highest Mach number reached in level flight during the tests was 0.49. Data of reference 8 show, however, that with war emergency power a Mach number of 0.54 can be reached in level flight with a Bell P-39N-1 airplane. With a Mach number of drag divergence of 0.62, the airplane could, therefore, be flown about 60 miles per hour faster than at present before the compressibility effect on drag would start to limit the high speed.

CONCLUSIONS

1. The minimum drag coefficient at low Mach number for the Bell P-39N-1 airplane was found to be approximately 0.022.

2. The Mach number of drag divergence (that Mach number at which the drag coefficient started to increase from its low-speed value) was 0.62.

3. The maximum Mach number attained in the course of the tests was about 0.80, which appears to be the terminal Mach number of the airplane. At this Mach number, the drag coefficient was about 0.060.

4. The slope of the curve of drag coefficient as a function of Mach number (dC_D/dM) in the high Mach number region was about 0.5.

5. The critical Mach numbers of the different airfoil sec-
tions of the wing as determined from pressure-distribution
measurements are, in general, in good agreement with the theo-
retical values of critical Mach number for the various airfoil
sections.

Ames Aeronautical Laboratory,
    National Advisory Committee for Aeronautics,
        Moffett Field, Calif.

APPENDIX A

Three methods are derived by which the airplane drag coefficient C_D may be obtained from flight-test data. The three methods are referred to as (1) the force method, (2) the energy method, and (3) the acceleration method.

Force Method

The drag of the airplane may be determined by use of records of altitude and airspeed. Equating the forces along the flight path (fig. 9) gives

$$F = T \cos \alpha + W \sin \theta - D$$

or

$$\frac{W}{g} a = T \cos \alpha + W \sin \theta - D$$

from which

$$D = T \cos \alpha + W \left(\sin \theta - \frac{a}{g} \right)$$

$$a = dV/dt$$

$$\sin \theta = - \frac{dh/dt}{V}$$

Substituting for $\sin \theta$ and $\frac{a}{g}$

$$D = T \cos \alpha - W \left(\frac{dh/dt}{V} + \frac{dV/dt}{g} \right)$$

or

$$C_D = \left[T \cos \alpha - W \left(\frac{dh/dt}{V} + \frac{dV/dt}{g} \right) \right] \frac{1}{qS}$$

where $\sin \theta$ and a are determined by graphical differentiation with respect to time, of altitude and velocity along the flight path.

Energy Method

This method involves the equating of the changes in potential and kinetic energy to the product of force and distance as follows:

$$d(work) = Fds = d(mgh) + d\,\frac{mV^2}{2}$$

$$= W\,dh + W\,\frac{V\,dV}{g}$$

$$= W\left(dh + \frac{V\,dV}{g}\right)$$

since

$$ds = V\,dt$$

and

$$F = T\cos\alpha - D$$

then

$$(T\cos\alpha - D)\,V\,dt = W\left(dh + V\,\frac{dV}{g}\right)$$

$$D = T\cos\alpha - \frac{W}{V}\frac{d}{dt}\left(h + \frac{V^2}{2g}\right)$$

and

$$C_D = \frac{T\cos\alpha - \dfrac{W}{V}\dfrac{d}{dt}\left(h + \dfrac{V^2}{2g}\right)}{qS}$$

It is seen that this method does not require the use of an accelerometer. The only instruments required are an altimeter and an airspeed recorder. The graphical differentiation of the quantity $(h + V^2/2g)$ with respect to time is required to evaluate the latter part of the right-hand term of the above equation. This equation is essentially the same result as is obtained by the force method, except that one graphical differentiation is required instead of two. The results obtained from the two methods differ only by errors due to the work-up of the basic flight data.

Acceleration Method

Determination of the drag of an airplane in flight may be made by consideration of the accelerations involved.

As before,

$$D = T \cos \alpha + W(\sin \theta - a/g)$$

$\sin \theta$ is measured by the components of the accelerometer due to their orientation in the gravitational field. Therefore

$$\sin \theta = A_{X_1} \cos \alpha + A_{Z_1} \sin \alpha$$

a/g is measured by the components of the accelerometer due to their acceleration along the flight path. Therefore

$$\frac{a}{g} = A_{X_2} \cos \alpha + A_{Z_2} \sin \alpha$$

hence

$$D = T \cos \alpha + W(A_{X_1} \cos \alpha - A_{X_2} \cos \alpha + A_{Z_1} \sin \alpha - A_{Z_2} \sin \alpha)$$

and since

$$A_X = A_{X_2} - A_{X_1}$$
$$A_Z = A_{Z_1} - A_{Z_2}$$

then

$$D = T \cos \alpha + W(A_Z \sin \alpha - A_X \cos \alpha)$$

or

$$C_D = \frac{T \cos \alpha + W(A_Z \sin \alpha - A_X \cos \alpha)}{qS}$$

APPENDIX B

The following discussion presents the method by which the drag coefficient at low Mach numbers was obtained from speed-power data. The method is based on the assumption that the airplane polar may be represented by a parabola in the normal flying range; for example, lift coefficients from 0.0 to 0.8.

The equation for the parabola is then written as

$$C_D = C_{D_p} + \frac{C_L^2}{\pi e A}$$

where

C_D total airplane drag coefficient

C_{D_p} effective parasite drag coefficient

e airplane efficiency factor

A aspect ratio

By proper mathematical manipulation, the following equation for indicated thrust horsepower required for level flight may be determined:

$$thp_i = thp(\sigma)^{1/2} = 6.82 \left(\frac{V_i}{100}\right)^3 f + \frac{0.332}{eV_i} \left(\frac{W}{b}\right)^2$$

where

f $C_{D_p} S$, sq ft

V_i $\sqrt{\sigma}$ V_{true}, mph

W airplane gross weight, lb

b airplane span, ft

The above-mentioned formula for the power-required term defines a single curve of indicated power required as a function

of indicated airspeed for all altitudes. By the proper appli-
cation of the foregoing formula, flight-test data may be re-
duced to give the airplane parameters e and f. This may be
accomplished by representing the power-required equation as
linear; that is, represented by the intercept equation of a
straight line

$$\frac{x}{a} + \frac{y}{b} = 1$$

where

$$x = \frac{1}{f}$$

and

$$y = e$$

Hence the power-required equation becomes

$$\frac{6.82 \, (V_i/100)^3 \, f}{thp_i} + \frac{0.332 \, (W/b)^2}{e V_i \, thp_i} = 1$$

If the values of $6.82 \dfrac{(V_i/100)^3}{thp_i}$ are plotted against values of

$\dfrac{0.332(W/b)^2}{V_i \, thp_i}$, then the intercepts of the line passing through

the given test points determine the equivalent flat-plate area
f and airplane efficiency factor e. In order to determine
the indicated thrust power, it is necessary to define the en-
gine brake horsepower by engine charts or a torquemeter, as the
case may be. From the power conditions (rpm, altitude, etc.)
the propeller efficiency may be determined and hence the pro-
peller thrust power. To this power must be added the exhaust
thrust power, if any. Exhaust thrust may be estimated by the
method of reference 3. By multiplying this value of thrust
power by $\sqrt{\sigma}$, the indicated power required (thp_i) is de-
termined, leaving only the gross weight and indicated airspeed
to be evaluated.

APPENDIX C

Propulsive efficiency was estimated from charts presented in reference 4 corrected for tip compressibility effects using the data obtained from reference 5. These data are presented in figure 10. The curves show the tip-speed factor η_t as a function of tip Mach number M_t for various advance-diameter ratios J. In using these curves the same critical tip Mach number was assumed to apply to the propeller on the Bell P-39N-1 airplane as applied to the test propeller of reference 5, since it was of the same thickness ratio and both propellers had high-critical-speed tip sections.

The compressibility losses over the blade root were estimated by the method developed in reference 6. The root corrections were then applied to the propeller efficiencies of reference 2 for power coefficients of 0.2 and 0.3, and for propeller tip Mach numbers of 0.8 and 1.2. These curves are shown in figure 11 as η_r, which is the ratio of propeller efficiency with root losses to propeller efficiency with no root losses. The over-all efficiency of the propeller was then calculated by multiplying the values of efficiency obtained from the chart of figure 10 and the chart of figure 11.

APPENDIX D

To establish the critical Mach number of the Bell P-39N-1 airplane wing, use was made of normal-force-distribution data at five spanwise stations along the wing. These data had been measured in flight in connection with a separate investigation on the airplane. The critical Mach number was determined at each section for the particular section lift coefficient corresponding to an airplane lift of 0.06, which is an average lift coefficient for the drag curves of figure 5. Since only normal-force-distribution data were taken, the flight data had to be reduced to pressures on upper and lower surfaces. This was done as is outlined in reference 9, which presents a method for the rapid calculation of the pressure distribution over an airfoil section when the normal-force distribution and the pressure distribution over the base profile (i.e., the profile of the same airfoil if the camber line were straight and if the resulting airfoil were at zero angle of attack) are known. Since there

were no pressure-distribution data available for base profiles
corresponding to the test sections, theoretical base-profile
pressure-coefficient distributions were used as determined from
the above-mentioned reference.

The resulting pressure distributions gave results which
checked very closely the value of critical Mach number as de-
termined by reference 10. The peak pressures at spanwise sta-
tions A, B, C, and D occurred between 10 and 20 percent chord,
hence the peak pressure was well defined. For station E,
which is approximately an NACA 23010 section, the peak pres-
sure occurs over an extremely limited portion of the airfoil
chord near the leading edge, and the relatively few orifices
near the leading edge prevented the peak pressures from being
accurately established. A value for the critical Mach number
for the tip section (station E) was arrived at, however, by
use of reference 10. Since the pressure-distribution data
from flight gave results that were in very close agreement with
the theoretical data for stations A, B, C, and D, it is thought
that the value of section critical Mach number for station E
is probably not greatly in error.

REFERENCES

1. Army Air Forces Specification No. C-619-21, Oct. 6, 1942.

2. Army Technical Order Series 01-110F-2, Aug. 30, 1944.

3. Pinkel, Benjamin, Turner, L. Richard, and Voss, Fred: De-
    sign of Nozzles for the Individual Cylinder Exhaust Jet
    Propulsion System. NACA ACR, April 1941.

4. Gray, W. H. and Mastrocola, Nicholas: Representative Oper-
    ating Charts of Propellers Tested in the NACA 20-Foot
    Propeller-Research Tunnel. NACA ARR No. 3I25, 1943.

5. Stack, John, Draley, Eugene, C., Delano, James B., and
    Feldman, Lewis: Investigation of Two-Blade Propellers
    at High Forward Speeds in the NACA 8-Foot High-Speed
    Tunnel. Part I - Effects of Compressibility. NACA
    4-308-03 blade. NACA ACR No. 4A10, 1944.

6. Hufton, P. A.: The Calculation of Airscrew Efficiencies
    at High Speed. B. A. Dept. Note Perf. 18, RAE, July
    1940.

7. Clousing, Lawrence A., Turner, William N., and Rolls, L.
   Stewart: Measurements in Flight of the Pressure Distri-
   bution of the Right Wing of a P-39N-1 Airplane at Several
   Values of Mach Number. NACA ARR No. 4K09, 1944.

8. Ivey, H. Reese, Stickle, George W., and Brevoort, Maurice J.:
   Performance Comparison of American Pursuit Airplanes.
   NACA CMR, Dec. 1943.

9. Allen, H. Julian: A Simplified Method for the Calculation
   of Airfoil Pressure Distribution. NACA TN No. 708, 1939.

10. Heaslet, Max A.: Critical Mach Numbers of Various Airfoil
    Sections. NACA ACR No. 4G18, 1944.

TABLE I.-TABULATIONS OF FLIGHT CONDITIONS DURING

HIGH-SPEED DIVES OF BELL P-39N-1 AIRPLANE

Dive number	Altitude		Maximum normal acceleration factor at pull-out (g)	Maximum Mach number attained	Engine conditions	
	At start of dive (ft)	After pull-out (ft)			rpm	Throttle setting
1	30,000	11,500	6.0	0.765	3050	Varied
2	28,000	10,300	4.4	.777	2800	Part
3	34,000	12,100	5.8	.797	3000	Full
4	32,000	22,000	5.0	.715	3000	Part
5	32,000	12,800	7.0	.785	2800	Part
6	30,000	10,000	4.6	.778	2600	Varied

NOTE: Oil and coolant shutter position for all dives;
one-half open (flush with external lines of fuselage).

A-61

13'-0"

34'-0"

NATIONAL ADVISORY
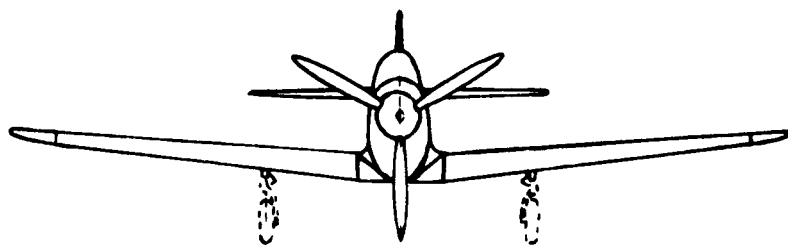COMMITTEE FOR
AERONAUTICS

30'-2"
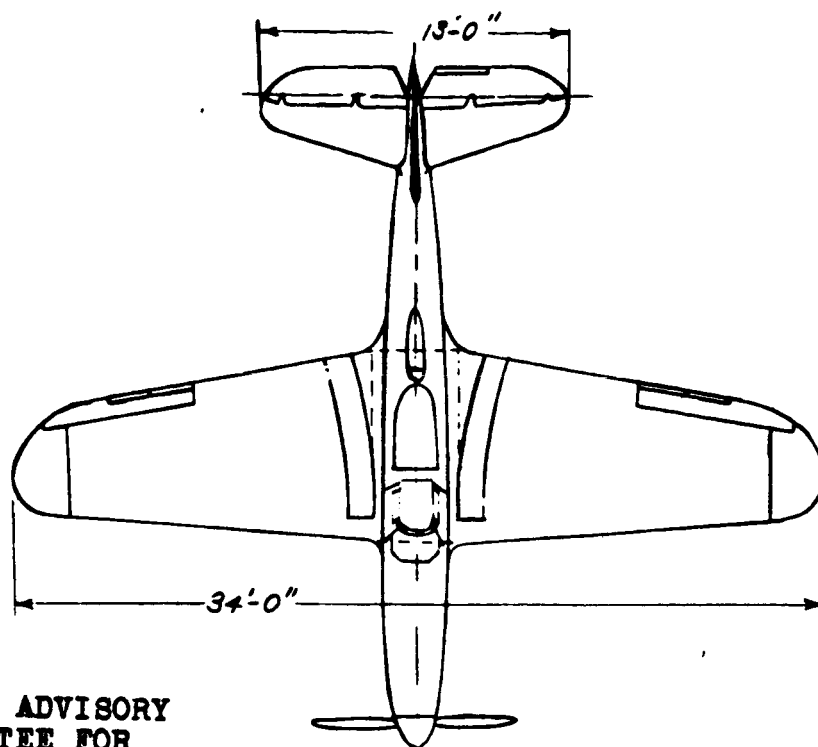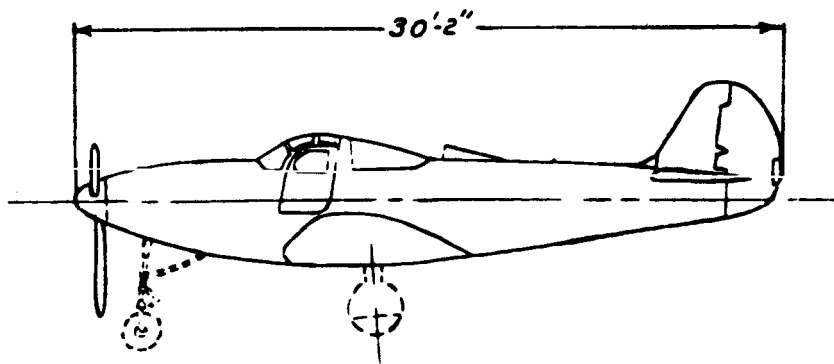
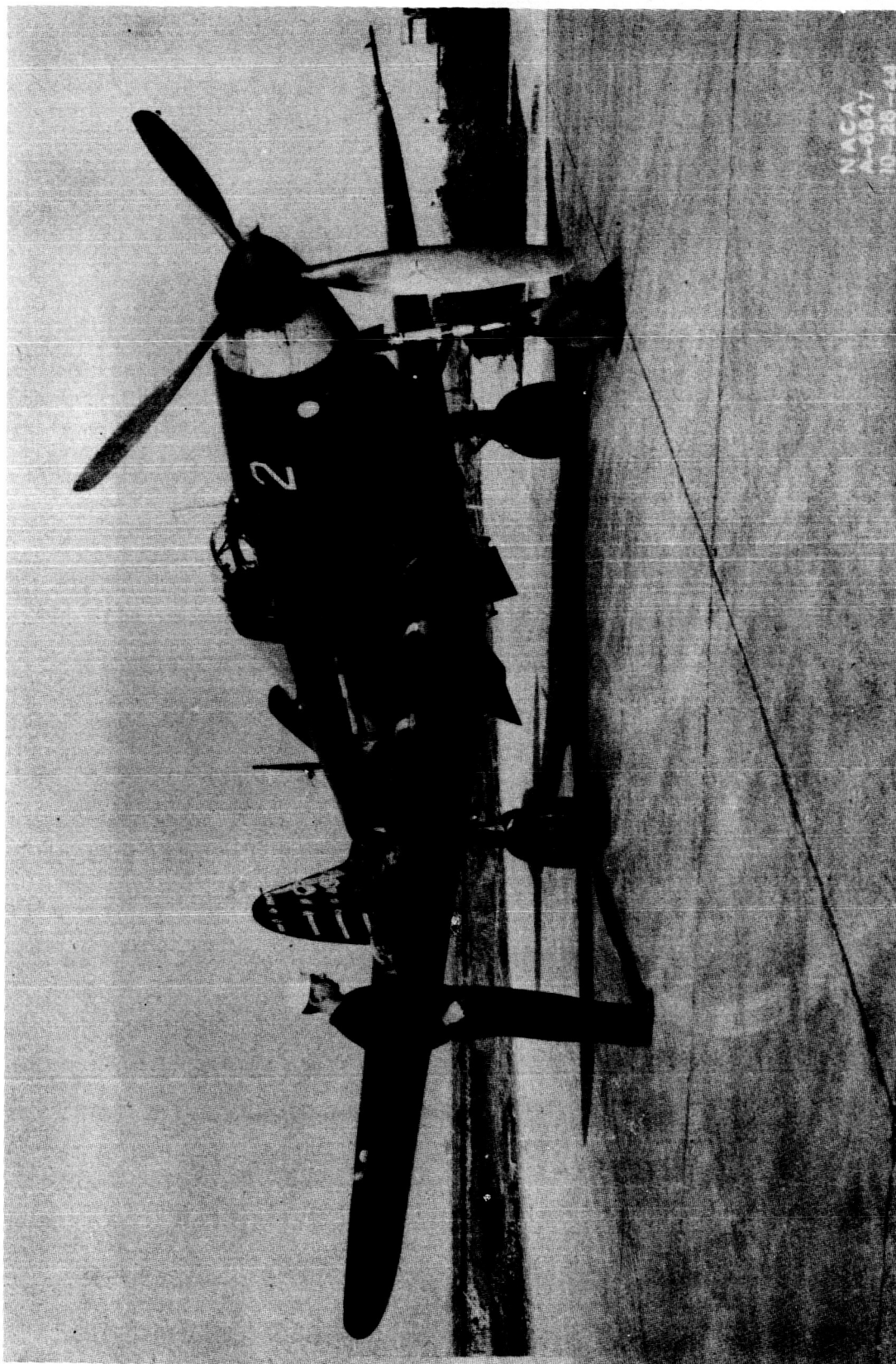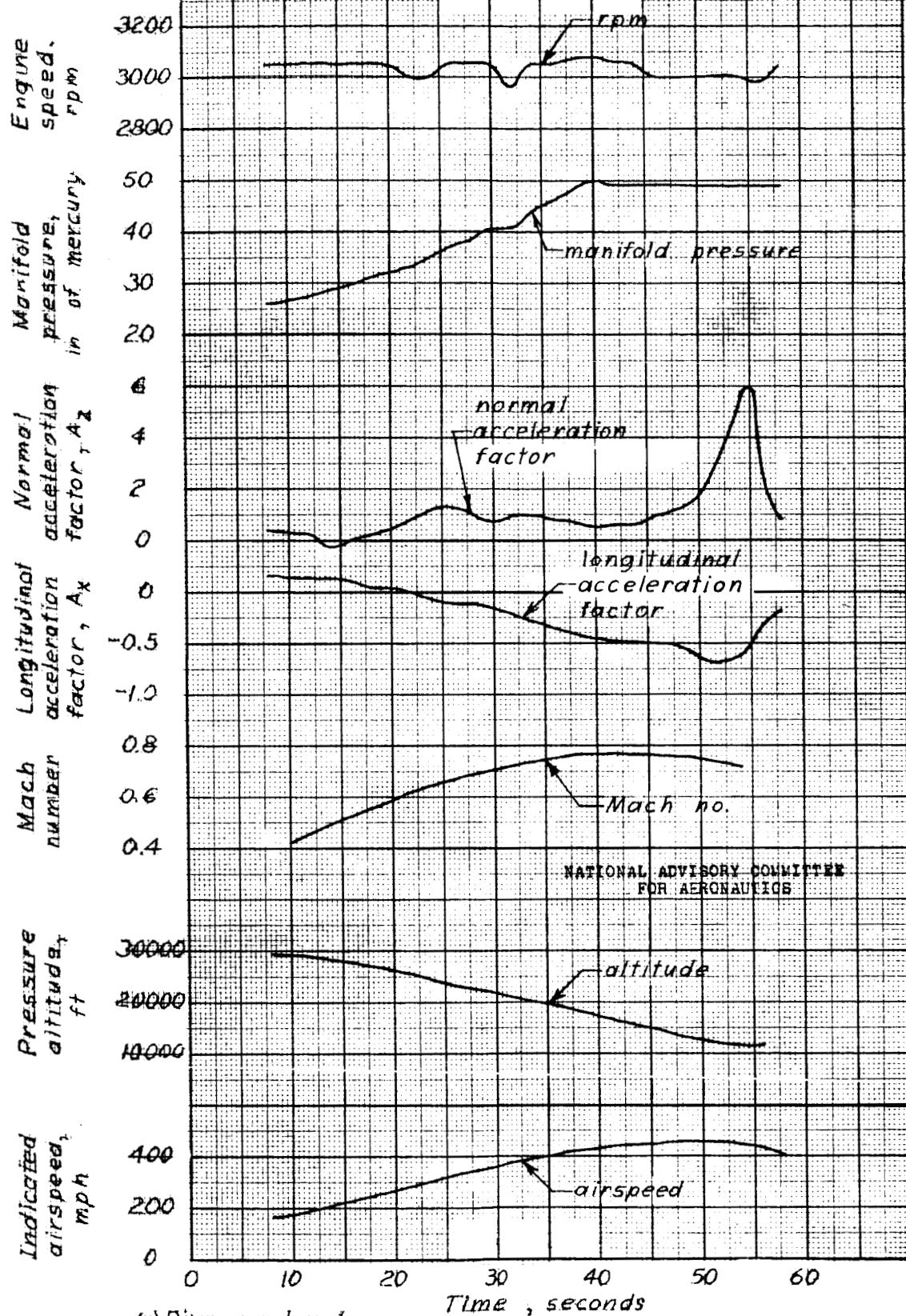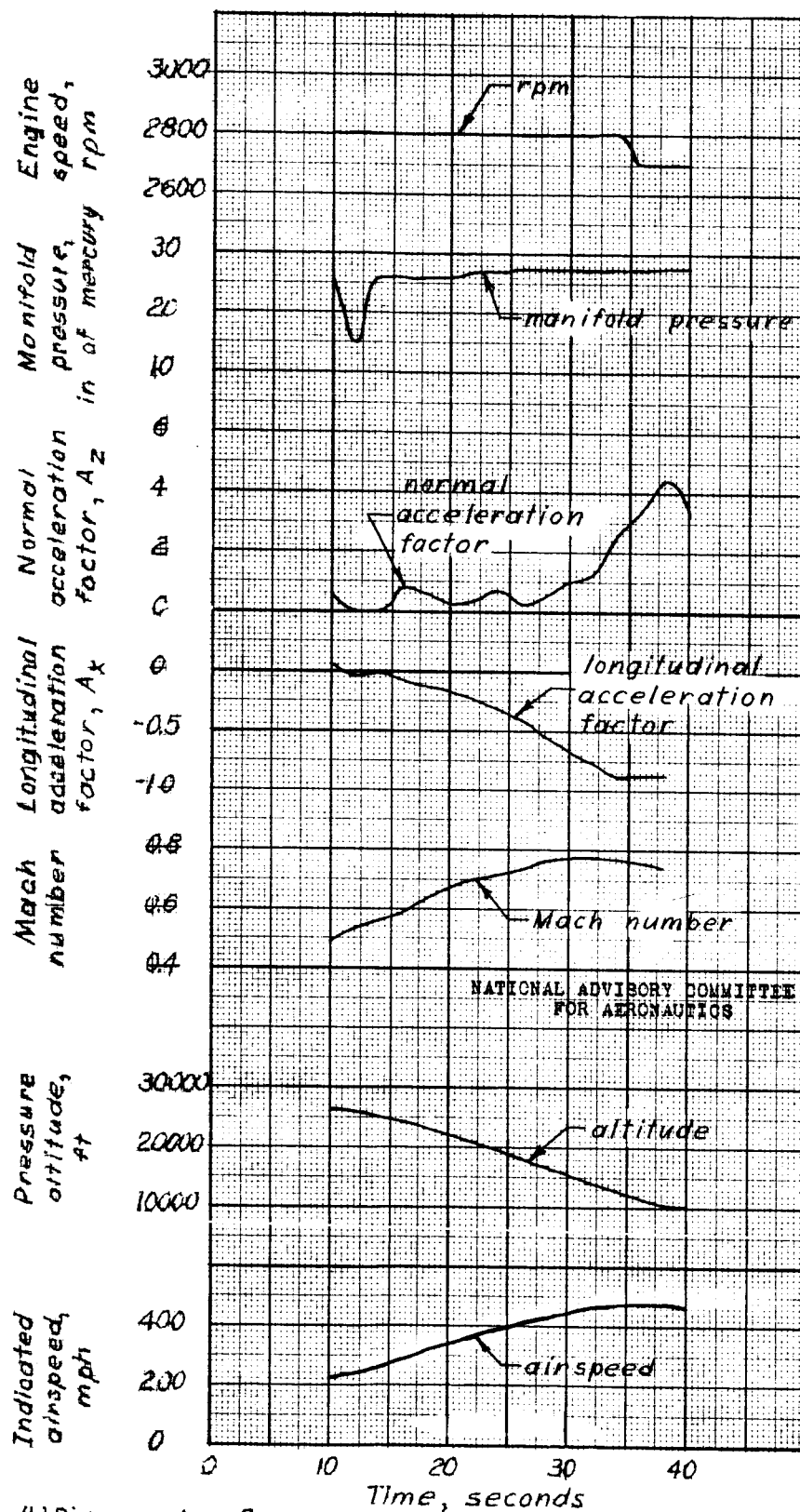Figure 1.- Three-view drawing of the Bell P-39N-1 airplane.

Figure 2.- Three-quarter front view of the Bell P-39N-1 airplane as instrumented for flight tests.

(a) Dive number 1

Figure 3— Time history of a power-on dive from 30,000 feet. Clean condition, oil and coolant shutters flush. Bell P-39N-1 airplane.

A-61

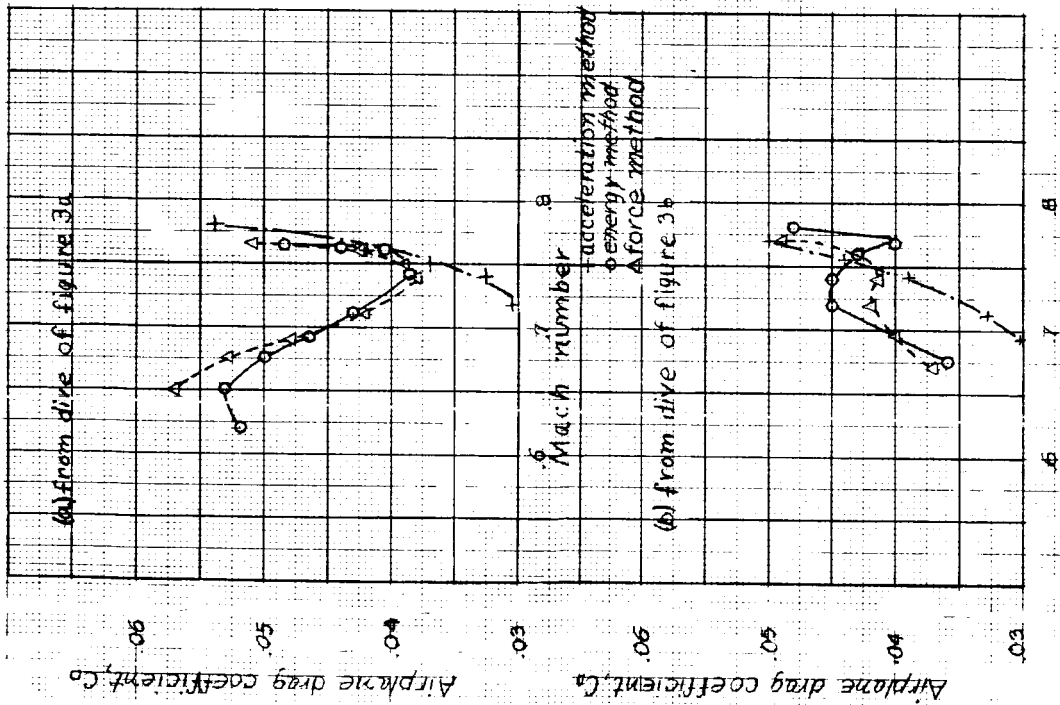(b) Dive number 2.

Figure 3. — Concluded.   Bell P-39N-1 airplane.

A-61

NATIONAL ADVISORY COMMITTEE
FOR AERONAUTICS

Figure 5.- Variation of airplane drag coefficient with Mach number as computed from level-flight data and from data taken during six dives, Bell P-39N-1 airplane.

Figure 4.- Comparison of the variation of airplane drag coefficient with Mach number as computed by use of the force, energy, and acceleration methods from measurements taken during two dives, Bell P-39N-1 airplane.

Figure 6.- Results of speed-power data run at 15,000 feet as plotted to determine the drag coefficient of the Bell P-39N-1 airplane.
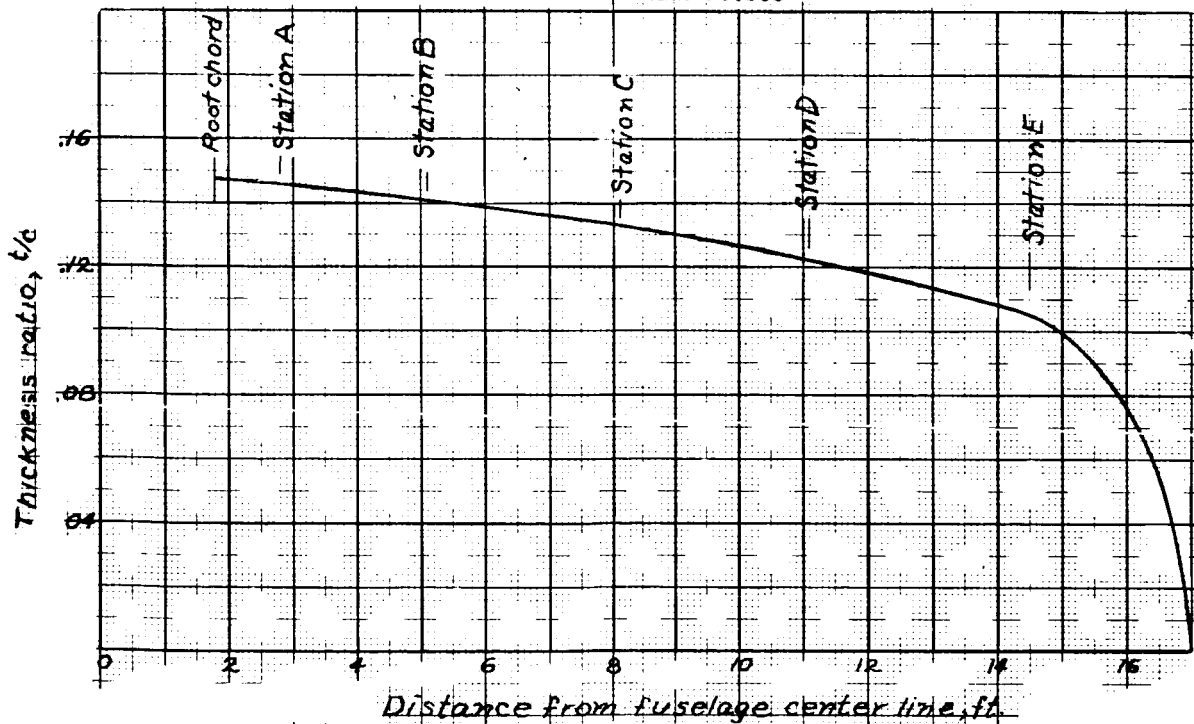
NATIONAL ADVISORY COMMITTEE
FOR AERONAUTICS

Figure 7.-Variation of thickness ratio along span of right wing Bell P-39N-1 airplane.
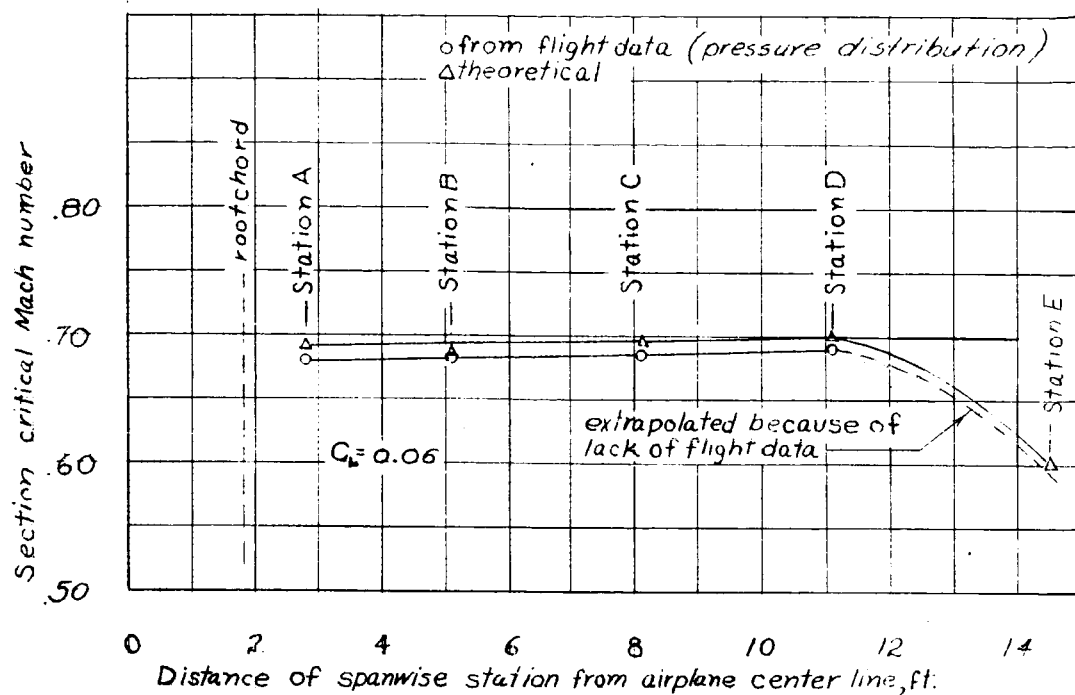
A-19

Figure 8.- Variation of section critical Mach number with span on the P-39N-1 airplane.
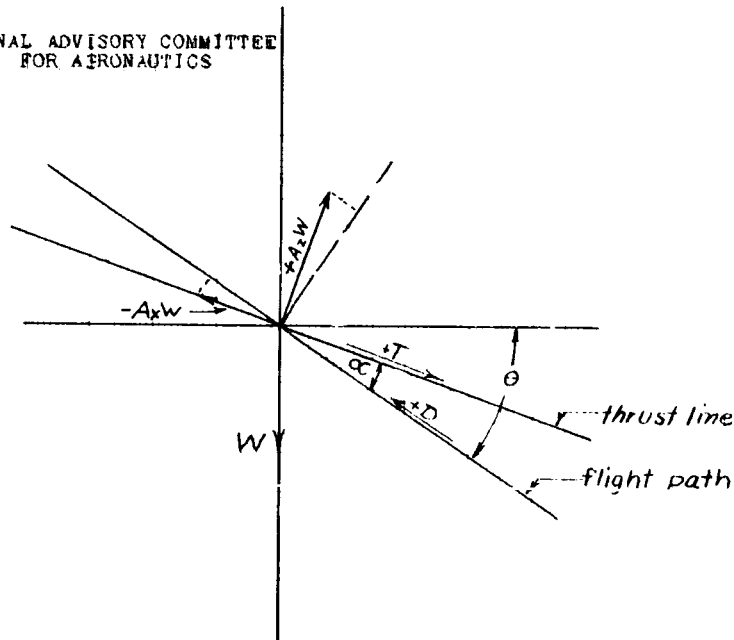
Figure 9.- Diagram of forces and accelerations acting at the center of gravity. Bell P-39N-1 airplane.

$M_t=1.2$

$M_t=1.1$

$M_t=1.0$

$M_t=0.9$

$M_t=0.3$

$C_p=.30$

$C_p=.20$

Airplane Mach number, M

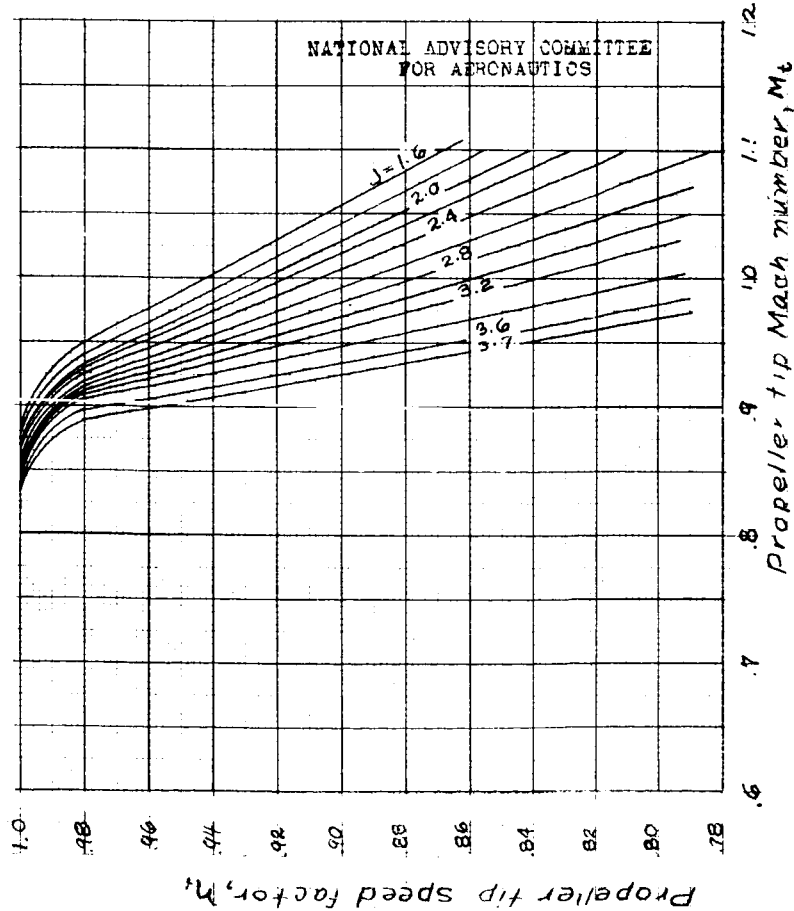Ratio of propeller efficiency with root losses to efficiency with no root losses, η_r

Figure 11.- Chart for correcting propeller efficiency for root losses on Aeroproducts A-20-156-17 propeller as installed on Bell P-39N-1 airframe.

NATIONAL ADVISORY COMMITTEE FOR AERONAUTICS

J=1.6
2.0
2.4
2.8
3.2
3.6
3.7

Propeller tip Mach number, M_t

Propeller tip speed factor, η_t

Figure 10.- Tip speed correction chart for Aeroproducts A-20-156-17 propeller on Bell P-39N-1 airplane.